CMLS, Cell. Mol. Life Sci. 59 (2002) 832–844
1420-682X/02/050832-13 $ 1.50 + 0.20/0

CMLS Cellular and Molecular Life Sciences

Review

Pore-forming toxins

R. J. C. Gilbert

Division of Structural Biology, Henry Wellcome Building for Genomic Medicine, University of Oxford, Roosevelt Drive, Oxford OX3 7BN (United Kingdom), Fax + 44 1865 287 547, e-mail: gilbert@strubi.ox.ac.uk
Oxford Centre for Molecular Sciences, Central Chemistry Laboratory, University of Oxford, South Parks Road, Oxford OX1 3QU (United Kingdom)

Received 7 September 2001; received after revision 12 November 2001; accepted 5 December 2001

Abstract. Pore-forming toxins are widely distributed proteins which form lesions in biological membranes. In this review, bacterial pore-forming toxins are treated as a paradigm and discussed in terms of the structural principles on which they work. Then, a large family of bacterial toxins, the cholesterol-binding toxins, are analyzed in depth to provide an overview of the processes involved in pore formation. The ways in which the cholesterol-binding toxins (cholesterol-dependent cytolysins) interact with membranes and form pores, the structure of the monomeric soluble and oligomeric pore-forming states, and the effects of the toxin on membrane structure are discussed. By surveying the range of work which has been done on cholesterol-binding toxins, a working model is elaborated which reconciles two current, apparently diametrically opposed, models for their mechanism.

Key words. Pore-forming toxin; cholesterol binding; membrane structure and dynamics; cryo-electron microscopy; pneumolysin; perfringolysin; streptolysin.

The evolution of compartmentalization, first as the cell and then within it, created a structural challenge in terms of communication through membranes. Pore-forming protein toxins are an aggressive further development, allowing pathogens to enter cells and/or damage or destroy them, for their own ends. The pore-forming toxins found in both prokaryotic and eukaryotic cells [1] are therefore analogous in function to antibiotics [2], components of the immune system [3], and the fusion proteins possessed by viruses [4, 5].

What is a pore?

It is important to be aware that the word ‘pore’ is a functional description and, therefore, that the actual structure a pore takes can be very different when generated by different means. For the purposes of this review, the function of a pore is to allow communication between two volumes previously separated by a biological membrane; typically, it will take the form of a water-filled lesion. However, what defines the extent of the pore and its lifetime are separate questions which have nothing to do with whether or not it qualifies as a pore. Thus, some proteins structurally define protein channels which function as pores [6–11] (fig. 1a, b) while fusion pores between membranes may be made exclusively of lipid [12, 13] or of a proteolipid complex [14] (fig. 1c). Fusion pores made of lipid alone could form spontaneously or with protein motive assistance [4, 5, 13]. Understanding that the structure of a pore does not have to be a protein channel is important to make sense of what might happen when a protein molecule changes the conductance properties of a biological membrane. Too much attention has been paid to rather static models for pore function, in which the pore is identified with a protein channel treated as a heterologous integral membrane protein, when the nature of lipid bilayers suggests much dynamic interac-

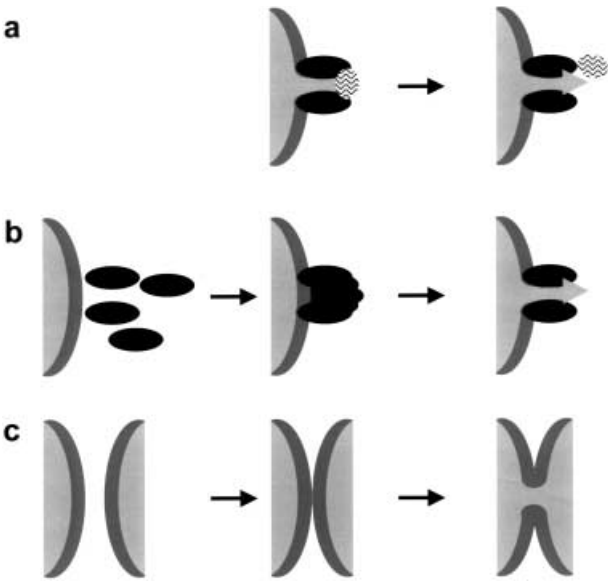

Figure 1. (*a*) Schematic representation of pore formation by an integral membrane protein. In a non-pore-forming state, the protein channel is blocked, but following a conformational change allows communication between the cell interior and the surrounding milieu. Some porins act in this manner. (*b*) Schematic representation of pore formation by a pore-forming toxin which ends in a structure resembling an integral membrane protein. Toxin monomers bind, oligomerize on the membrane surface, and then insert to form a conducting channel. This is the kind of mechanism adopted by *Staphylococcus aureus* α toxin. (*c*) Schematic representation of pore formation by membrane fusion. In this case, the membranes become confluent, thus providing a physical passage between two volumes.

tion would occur between membranes and proteins forced into them [15]. We call the proteins *toxins* because they adversely affect membrane function; this observation highlights another factor which may be important for an accurate perspective on some of these proteins, that the pores may exist for rather short periods of time before the cell or other membrane into which they have inserted is completely destroyed.

How widely distributed are pore-forming toxins?

Proteins which form pores have been identified in a wide range of organisms including bacteria, plants, fungi, and animals, and in some cases show mechanistic and structural homologies across vast evolutionary distances. For example, a pore-forming toxin from the sea anemone *Metridium senile* appears to be very like the members of a family of cholesterol-binding toxins produced by bacteria in the morphology of its pore-forming oligomers and dependence for membrane damage on the presence of cholesterol in the target membrane [1]; furthermore, the pore-forming toxin enterolobin from the Brazilian plant *Enterobium contortisiliquum* displays significant sequence homology (45% identity, 60% similarity) to aerolysin, the pore-forming toxin of the bacterium *Aeromonas hydrophila* [16–18]. However, for practical reasons, as well as a concern for their disease-causing abilities, the pore-forming toxins of bacteria have received far more attention than those from any other kind of organism. By studying bacterial toxins we can understand much about other pore-forming proteins through the general principles they reveal and on the basis of the homologies just noted. Pore-forming bacterial proteins have been covered extensively in the literature, including a number of good reviews such as those by Bhakdi and colleagues [19], Hughson [20], Lesieur and colleagues [21], Gouaux [22], and Alouf [23]. I will briefly summarize them here, before moving on to a discussion of one large family of bacterial pore-forming toxins which are dependent for their action on the presence of cholesterol in the target membrane. This family of cholesterol-binding toxins (CBTs) [23, 24] stands as a paradigm for research into the action of pore-forming proteins which combines a wide range of techniques to investigate the structural, mechanistic, and dynamic aspects of their activity.

Bacterial pore-forming toxins

Bacterial toxins which form pores can be broadly classified into two groups, those which are thought to interact with the membrane through α helices and those which utilize mostly β sheet structures such as β barrels. This dichotomy has in particular been noted by Lesieur and colleagues [21] and by Gouaux [22]. Since structural analysis holds the key to understanding mechanism, it will be used to systematize our discussion. The helical family includes the AB_5 family of toxins, *Bacillus thuringiensis* δ endotoxins, and the bacterial colicins such as colicin Ia of *Escherichia coli* [for reviews see refs 20, 25, and 22]. Examples of AB_5 toxins are the heat-labile enterotoxins of *Vibrio cholerae* (the causative agent of cholera), *Shigella dysenteriae* (dysentery), *Bordetulla pertussis* (whooping cough), and enterotoxigenic *E. coli*. The B subunit is pentameric and confers receptor binding and thereby cell specificity, and is crowned by the A subunit which is an ADP-ribosylase [26, 27]. The *B. thuringiensis* δ endotoxins are agriculturally important insecticidal agents [28–30] which are thought to act through oligomerization [22]. Colicins are agents of bacterial warfare which kill sensitive strains of *E. coli*; their mechanism is a matter of controversy [21, 31].

The structural basis of pore formation is much better characterized for a number of the toxins which interact with membranes through β sheet conformations. Members of this class include aerolysin from *A. hydrophila* (fig. 2a), α toxin of *Staphylococcus aureus*, the protec-

tive antigen (PA) of *Bacillus anthracis* (fig. 2b), and the CBTs produced by various bacterial genera [for reviews see refs 32–34]. Aerolysin, α toxin, and PA all produce heptameric channels [6, 35, 36] which form the toxin pore [7, 36]. The bi-component leukotoxins are closely related structurally to α toxin, and through solution of representative structures for them, both soluble monomeric [37, 38] and detergent-solubilized heptameric [6] atomic models have been derived for the α-toxin-like family (fig. 2c). However, the leukotoxins themselves may form rather larger pores than α toxin [39]. Functional experiments have indicated a bimodal distribution of pore sizes for α toxin; the use of molecular modeling procedures replicated the observed conductances of the two forms in silico and suggested that α toxin forms functional hexamers as well as heptamers [40]. In connection with this, it is worth observing that an even-numbered oligomer is easier to reconcile with the bi-component activity of the leukotoxins than an odd-numbered one [41]. The best candidate currently for biotechnological application of pore-forming toxins in signaling the presence of particular chemicals or in controlling membrane permeability is *S. aureus* α toxin [7, 42, 43].

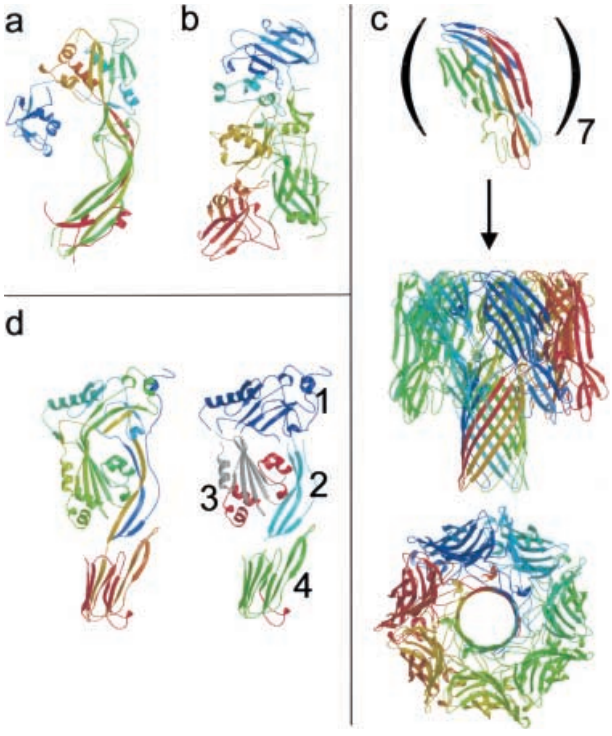

Figure 2. (*a*) The structure of monomeric aerolysin colored in a rainbow ramp from blue at the amino terminus to red at the carboxy terminus [36]. (*b*) The structure of monomeric protective antigen colored as in (*a*) [35]. (*c*) At the top, the structure of staphylococcal leukocidin LukF colored as in (*a*), respresentative of the monomeric form of the heptamerizing α-toxin-like pore formers [38]; below, the structure of heptameric staphylococcal α toxin in two orientations [6]. The 'stalk' region of this 'mushroom' is transbilayer. (*d*) Two views of the perfrinoglysin monomer solved by X-ray crystallography [45]. On the left, the molecule is colored as in (*a*). On the right, the four domains are colored differently: domain 1 blue, domain 2 cyan, domain 3 gray, and domain 4 green. The regions of domain 3 involved in pore formation are shown in red, as is the hook-shaped loop in domain 4 which is involved in binding events. All the molecules in this figure are displayed on the same scale.

Although their oligomers are heptameric, the structure of the toxin protomer is very different for aerolysin, PA, and α toxin (fig. 2a–c). With α toxin and PA, each monomeric subunit contributes one β hairpin to a β barrel, which is inserted through the membrane [6, 35]. The hairpin is formed from a β structure in α toxin [6, 37, 38] and from a disordered loop in PA [35]. With aerolysin, the number of transmembrane hairpins is unknown, but has been variously estimated at two, three, or four [22]. CBTs contrast strongly with these other toxins in forming large ring- and arc-shaped oligomers with up to 50 subunits; the trans-membrane region of CBTs is believed to consist of a gigantic β barrel to which each subunit is thought to contribute at least two hairpins [44]. In the soluble monomeric structure, these hairpins form six short α helices [45]. The use of two β hairpins to span a membrane is reminiscent of the structure of *E. coli* TolC, an outer membrane protein facilitating direct communication between the bacterial cytoplasm and its environment [11]. The usefulness of this comparison is limited, however, because TolC is a completely different entity – an integral membrane protein forming a rather narrow trimeric channel [11].

The proposal that CBTs use a helical-to-sheet conversion to transform from a soluble to a membrane-inserted form has the implication that where the structure of a monomeric protein is helical, the structure of its membrane-interacting portion may be sheet (and vice versa?). Thus the structural division just summarized may be erroneous. An interesting aside connected to this point concerns the recently characterized HlyE family of toxins with known representatives in *E. coli*, *Salmonella typhi,* and *Shigella flexneri* [46, 47]. The structure of HlyE from *E. coli* is distinctive, elongated, and helical save for a single β hairpin (the 'β tongue') [47]. HlyE has been shown to oligomerize during pore formation; the location of the β tongue at one end of the molecule and its hydrophobic character suggest it is the region which interacts with the interior of the lipid bilayer [47].

Cholesterol-binding toxins

Structurally and functionally related CBTs (also known as thiol-activated toxins and cholesterol-dependent cytolysins) have been identified in five genera of bacterium: *Streptococcus*, *Listeria*, *Clostridium*, *Bacillus,* and *Arcanobacterium* [48, 49]. A number of reviews have appeared on CBTs, including those by Alouf and Geoffroy

[48, 50] and Tweten and colleagues [44]. A particularly good review is that by Morgan and colleagues [51], which is unusual in giving due emphasis to the actual role of the CBTs in disease. Prominent CBTs include streptolysin from *Streptococcus pyogenes*, perfringolysin from *Clostridium perfringens*, listeriolysin from *Listeria monocytogenes,* and pneumolysin from *Streptococcus pneumoniae*. Streptolysin is widely used for permeabilizing cell membranes as a research tool [52], although consideration of the more complex effects brought about by CBT action on cells should occasion pause for thought about this [51]. In general, CBTs are thought to act on the cholesterol-containing cell membranes of nucleated cells, but an exception is listeriolysin which has a different pH/activity profile to the other toxins and mediates intracellular growth of *L. monocytogenes* by releasing it from phagosomes [53–55]. Pneumolysin also differs from the other CBTs in only being released on bacterial cell lysis – this is thought to relate to the pathogenic mechanisms of pneumococci [51].

How CBTs work

The prerequisite for a CBT to attack a membrane is the presence in it of cholesterol [48, 56, 57]. The ability of the CBTs to actually bind cholesterol has been visually demonstrated [58] and we will assume that cholesterol is a receptor if not the receptor, since the evidence for this is entirely compelling [48, 59, 60]. Nevertheless, the question of CBT receptor identity has recently been reviewed and the possibility of other important factors in toxin binding raised [44]. There appear to be two classes of CBT-binding site, with dissociation constants of 100 nM and 1 nM, found in both authentic cell membranes and synthetic liposomes [61]. The fact that the same two classes of binding site are found in liposomes and cell membranes supports the idea that cholesterol itself is the receptor; if something specific to cell membranes were the receptor, then patterns of binding to cells could not be replicated in synthetic liposomes. The low-affinity binding sites greatly outnumber the high-affinity ones [61], while the cholesterol in each kind of binding site is differently exchanged or oxidized [61, 62]. Furthermore, the lengths of the fatty acid chains in the phospholipids present in the membrane affect the appearance of high-affinity sites. The presence of carbon-18 fatty acids induces the presence of high-affinity cholesterol binding sites, which appear above defined threshold cholesterol concentrations [61]. As the mole percentage of cholesterol present in the liposome increases, so does the number of high affinity binding sites, and higher carbon-18 concentrations lower the threshold for their appearance (see table 1) [62]. The presence of carbon-carbon double bonds, which lengthen acyl chains, also promotes binding of

Table 1. Relationship of fatty acid chain length to the appearance of high-affinity CBT-binding sites in cholesterol-containing liposomes [data from ref. 62].

Ratio of fatty acyl chain lengths in lipsome (carbon-16: carbon-18)	Threshold for appearance of high-affinity binding sites (mole % cholesterol)
1.00	43
0.50	40
0.38	40
0.09	36
0	31

Data from Ohno-Iwashita et al. [62].

CBTs [63]. One possible high-affinity binding site which would be favored by these factors is a tail-to-tail trans-bilayer cholesterol dimer, in which case, the low-affinity binding site would be monomeric cholesterol dissolved in the membrane. This suggestion is supported by the fact that pneumolysin, and polyene antibiotics, which have been shown to bind trans-bilayer cholesterol dimers preferentially [64], interact with cholesterol crystals in the same way [unpublished result; 65, 66].

After binding membranes, CBTs oligomerize into arc- and ring-shaped oligomers in or on the lipid bilayer, leading to the formation of a pore. The oligomers formed by CBTs may have up to 50 subunits; the arc-shaped oligomers are incomplete rings and have the same curvature [67–69]. The mechanism by which oligomerized CBTs form pores is the subject of intense discussion, involving apparently diametrically opposed viewpoints [44, 69–71]. One is that oligomerization to a ring-shaped complex is complete before pore formation occurs [44] (the proponents of this theory refer to the membrane-bound complex not forming a pore as a 'prepore,' following the conceptual framework for toxin pore formation developed for *S. aureus* α toxin [6]); the other theory is that pore formation is simultaneous with oligomerization, and that the arcs are themselves pore forming [67, 69]. In fact, the data support a hybrid model of the two which will be discussed in detail below. It is first necessary to describe the structure of a CBT and its oligomeric forms, and experimental results which have provided insights into characteristics of pores formed by CBTs and the regions of their structure involved in each stage of their activity.

The structure of a CBT

Solving the X-ray crystal structure of a CBT (perfringolysin) revealed that it has an elongated, four-domain structure [45]. The N-terminal 75% of the molecule contains three domains, with the polypeptide chain passing backwards and forwards between them; the fourth, C-

terminal domain, is discrete and has an immunoglobulin-type fold (fig. 2d). There are no pronounced areas of hydrophobicity on the structure and, thus, it is unclear how it inserts into a membrane. The receptor-binding region of the toxin, located largely on the basis of mutagenesis data, is in the C-terminal fourth domain [44, 45]. This domain also contains the most conserved portion of the CBTs, an undecapeptide which appears from mutational and other studies to be a key player in toxin activity [55, 60, 72–75]. The undecapeptide region possesses an unusual hooked loop structure that has been proposed to act as a 'dagger' to insert into the surface of the lipid bilayer and interact with cholesterol [45, 76]. The fourth domain apparently inserts rather shallowly in the membrane during pore formation: the inserted region includes part of the undecapeptide, quite possibly in a 'dagger' rather than a 'hook' conformation [76–78]. A particularly interesting mutant in the undecapeptide is a Trp433Phe substitution made in pneumolysin, which paradoxically alters the size distribution of pores such that they tend to be larger, although the cytolytic activity of the toxin is lowered by 99% [60].

A second region of CBTs implicated in their cytotoxic mechanism is in domain 3 [44, 79], meaning that CBTs are thought to interact with membranes using two domains. Toxin mutants were made which contained a single cysteine at a series of different positions [80]. Derivatizing the cysteine of each mutant with the fluroscent dye N′-dimethyl-N-(iodoacetyl)-N′-(7-nitrobenz-2-oxa-1, 3-diazolyl)ethylenediamine (NBD) allowed the polar or apolar environment of each mutated residue to be monitored during pore formation as reported by polarity-induced changes in the fluorescence of the dye. NBD was a particularly good choice for this because the lifetime and intensity of its fluorescence emission increase substantially on passing from an aqueous to a hydrophobic milieu. The local environment of NBD was monitored on the basis of the emission lifetime and intensity and collisional quenching of its fluorescence. The quenching agents were either iodide (in the aqueous phase) or nitroxide attached to the phospholipid acyl chains [80]. The environment of residues within a region of domain 3 consisting of three small α helices alternated in the pore-forming state of perfringolysin between hydrophilic and hydrophobic environments, strongly suggesting their formation of an antiparallel amphipathic β hairpin [80]. Later, a second region of domain 3 also consisting of three small α helices was identified by similar methods as forming a second antiparallel amphipathic β hairpin [71]. These two β hairpins in combination with those from other monomers are thought to form the wall of a large β barrel at the interface between the membrane and an aqueous pore [71, 80]. Thus, while domain 4 mediates membrane binding, domain 3 is key in pore formation.

Tweten and co-workers have also addressed the temporal arrangement of these interactions using fluorescence spectroscopy as above and some elegant site-directed mutagensis which allows conformational locking of domain 3 to domain 2 [81]. This work showed that the fourth domain binds to the membrane and that domain 3 then inserts, and that this sequence is always followed. It furthermore confirmed that pore formation arises from domain 3 insertion, and that binding and pore formation were dependent on the presence of cholesterol in the membrane [81]. These experiments also served to confirm that domain 4 did not enter far into the membrane [77, 78], and suggest that the regions of domain 4 which affect the characteristics of pores formed by CBTs do so via some effect they have on the membrane insertion of domain 3. The ability to link reversibly domain 3 to domain 2, and thereby block and then unlock its pore-forming activity after oligomerization, demonstrated that oligomerization is the rate-determining step in pore formation and that the oligomer formed on the membrane surface prior to insertion is a genuine intermediate in it [70, 82].

Oligomerization by CBTs does not require membrane or cholesterol binding, although it is greatly assisted by it. Investigating the solution state of pneumolysin using analytical ultracentrifugation has shown that the toxin exists in a dynamic equilibrium between monomeric and dimeric forms [83, 84]. Therefore, self-interaction is an innate capability of CBTs: chemical derivatization and mutagensis studies have shown that the primary self-interaction is mediated through domain 4 [83, 84]. Other work with streptolysin has re-iterated this finding [85]. Pneumolysin also activates complement, in a non-immunospcecific manner involving domain 4 and interaction with the Fc region of IgG [86]. Since Fc and the CBT fourth domain are similar in structure, self-recognition and homo-oligomerization of pneumolysin have been suggested to be a related phenomenon to complement activation [76, 83, 84]. If this is so, then the other CBTs, being structurally homologous, would also be expected to activate complement directly.

At higher concentrations, pneumolysin forms oligomers of both ring and arciform types in solution [83]. The oligomers are morphologically very similar to those observed in membranes [83]. At very high toxin concentrations and in particular in the presence of ^2H_2O, pneumolysin has been shown to form helical oligomers [83], which proved very useful for structural analysis [87]. The formation of helices also bears out a mechanistic point: that oligomerization is driven – or stopped – by toxin concentration effects. Helicization demonstrates that in situations where the toxin is at very high concentrations, the oligomerization process does not terminate in a ring. Instead, the natural curvature (also evident in arcs having the same curvature as rings) and unnatural length of these oligomers give rise to helices.

The sizes of the pores formed by CBTs vary widely and form in discrete (all-or-none) steps [60, 88, 89], and this appears to be reflected in the presence of pore-forming arcs as well as rings [67, 68]. Discrete step-like pore formation supports the single transition model of Tweten and colleagues (fig. 3a), but the variability of pore size indicates that the surface-bound intermediate is not always a full ring oligomer, although of course it can be. A particularly neat demonstration that small oligomers form small pores was made by Palmer and colleagues [69] working with streptolysin. These authors showed that mixing a mutant that apparently 'capped' oligomerization with native toxin gave rise to a higher population of smaller (arc-shaped) oligomers, and that these oligomers formed smaller functional pores. The interpretation given to these data was that CBTs insert fully into the membrane and form pores at an early stage in oligomerization, and that increase in size of the oligomers is co-terminous with increase in pore size. In this interpretation, the pore lesion is created between the arc and a free edge of lipid which lengthens as the arc forms a half-ring and then shrinks as the ring is completed, to be finally excluded, leaving a protein channel through the membrane as in the final state envisioned by Tweten and colleagues [44, 67, 69] (fig. 3b). The Tweten model (fig. 3a) involving complete oligomerization prior to pore formation, and the Palmer model (fig. 3b) in which pore formation and oligomerization are simultaneous, can be combined to explain the data of both if membrane-bound arcs can also insert and form pores (fig. 3c). Combining the two models is a simple elaboration of either, merely requiring the acceptance that both lines of enquiry are providing genuine insights into CBT pore formation, despite the differences in the experimental methodology employed and the possible attenuation of toxin activity due to mutation or the binding of fluorescent dyes. If a toxin form still causes leakage/pore formation, then concluding that measurements made from it relate to the activity of wild-type toxin is entirely reasonable.

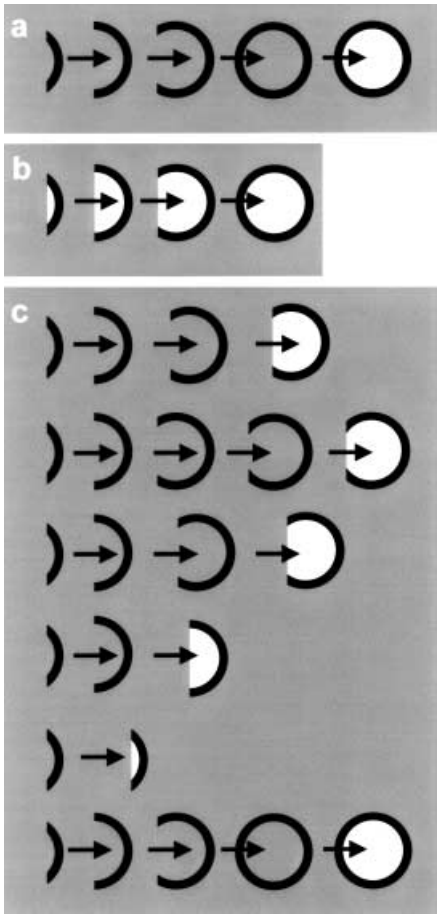

Figure 3. Schematic views of pore formation seen from above. The membrane surface is shown in gray and the oligomer in black; the pore is white. (*a*) The scheme favored by Tweten and colleagues, in which oligomerization to a ring-shaped surface-bound complex occurs before pore formation. (*b*) The scheme favored by Palmer and colleagues, in which oligomerization and pore formation are simultaneous, with the arcs forming pores completed by a lipid edge. (*c*) A combined model proposed here in which surface-bound oligomers form before inserting to create pores, but the transition between the two states can occur with arc surface-bound oligomers as well as ring-shaped ones.

Pore formation by CBTs according to a combined model would occur in the following critical stages: (i) binding; (ii) oligomerization in a concentration-dependent manner on the surface of the membrane into a surface-bound oligomer – when concentration becomes limiting, pore formation occurs as a result of (iii) insertion of part of domain 3. In this scheme, all oligomeric intermediates are capable of membrane insertion while oligomerization after insertion is impossible [41], with the size of the pore population formed consequently being a competition between growth rate and insertion. Given the electron microscopical evidence [67–69], the locking/unlocking of pore formation and its separation from cell binding and oligomerization [70, 81, 82], the definitive demonstration that small oligomers form small pores [69], and the fact that pore size varies widely and pores open in a quantized fashion [60, 88, 89], this seems a highly plausible scheme. If concentration is not limiting, then full rings will tend to form [82]; if it is limiting or the oligomerization is prematurely terminated, then more arcs will tend to form, resulting in more smaller pores [69]. Since it has been calculated that only 10–100 CBT monomers are required for cell lysis to occur [48], and given that the toxin concentrations during infection will be much lower than those used in vitro, smaller (arc-formed) pores may well be more important in destroying host cells than ring-formed pores. If pores of smaller size, perhaps forming rather rapidly, are the key elements in cell damage in vivo, then this could explain why, although it forms more larger pores than wild-type toxin, the pneumolysin mutant Trp433Phe has 1% normal cytolytic activity [60].

The oligomerization and pore-forming process involves a series of conformational changes in CBTs. The structures of these conformations will be described below. First, I will address the structure of the membrane that is under attack, which is particularly interesting given that pore formation by arcs apparently calls for the structural lesion to be completed by a wall of lipid [67, 69].

The structure of the membrane

Monitoring the changes in lipid bilayer structure that occur when CBTs form pores has involved an analogous technique to fluorescence spectroscopy, solid-state nuclear magnetic resonance (NMR) [90]. Both techniques rely on spectroscopic reporters to indicate the chemical environment of molecules; in the former case, it is the fluorescence-modifying nature of the environment, in the latter, the way in which it modifies nuclear spin. Another technique which could be used to study membrane structure under toxin attack is electron spin resonance (ESR) [91].

Different arrangements of phospholipids have characteristic ^{31}P NMR spectra due to having characteristic motional properties, and therefore any effects of a CBT on the bilayer structure will be reflected in an altered spectrum. The use of solid-state NMR to monitor the effects of pneumolysin on liposomal membranes has indicated dramatic cholesterol- and concentration-dependent changes in the distribution and organization of phospholipids [92, 93]. In the absence of pneumolysin, cholesterol-containing liposomes used in this work displayed an NMR spectrum typical of a bilayer. When toxin was added, the lipids divided into two different populations: one again showed a bilayer spectrum where the principle axis of phospholipid motion is coaxial with its acyl chain, but within smaller vesicles than the initial preparation. The other showed a spectrum typical of an inverted hexagonal phase in which the principle axis of motion of the phopholipids is perpendicular to their molecular axis. Electron microscopical evidence and the motional properties of the complexes displaying the inverted-hexagonal-like spectrum indicate they are most likely to be free oligomers with an outer belt of lipid. Pneumolysin also appeared to cause liposome aggregation/fusion. Overall, the solid-state NMR experiments indicate that the following changes occur in membrane structure when CBTs form pores within them: (i) liposomes fuse to form large membranous compartments with oligomers inserted into their bilayer; (ii) some oligomers with lipid bound enter free solution; (iii) small protein-free vesicles are pinched off in the fusion/oligomer-shedding process. An important role for the formation of structures with inverted-hexagonal-type NMR spectra during CBT-induced lysis is supported by the finding that streptolsyin activity is enhanced by cone-shaped lipids [94], since these are exactly those lipid molecules which have a propensity to form inverted hexagonal phases [95].

Membrane structure during pore formation by pneumolysin has also been studied using small-angle neutron scattering (SANS) [84]. Whereas solid-state NMR provides information on the environments inhabited by phospholipids, SANS gives structural insights into the overall changes in membrane structure during pore formation. SANS data were collected from liposomes, liposomes in the presence of active pneumolysin, liposomes in the presence of pneumolysin inactivated by thiobenzylation of the cysteine within the conserved CBT undecapeptide, and this last sample after activation by dithiothreitol. Pneumolysin appeared to associate with the liposome membranes even when inactivated by benzylation, and this resulted in the membrane appearing thicker than in the liposomes alone. Activation of the toxin or the presence from the start of active toxin caused the membrane to become thinner again. These results suggest that binding may be a two-stage process, resolved by derivatization of the undecapeptide cysteine, and that CBTs may alter the structures of the bilayers within which they reside. The thinning of the bilayer may be related to the formation of free oligomer-lipid complexes with inverted-hexagonal-like lipid motional properties, since it is known from other systems that thinning contributes to the formation of such structures by pinching lipid headgroups closer together [96]. A possible structure for the lipid edge purported to close pore-forming arcs of CBT oligomer is similar to inverted-hexagonal-phase tubes, fused with a bilayer [67, 69]. Hence the SANS work sheds light on the problem of what the structure of a lipid wall completing a toxin pore partially edged with protein might be, as well as on the appearance of free-floating oligomer/lipid complexes, and suggests they are related phenomena. Both the SANS and solid-state NMR experiments were carried out using toxin at defined toxin:cholesterol ratios and indeed monitored the effects of rising pneumolysin concentration on the transitions in membrane structure observed, detecting a steady rise in the lipids entering novel phases with rising toxin concentration [84, 92, 93]. Given that the lowest toxin concentration used in these experiments was 0.5 Molar % of the cholesterol concentration in the system, which is similar to the concentrations (0.1 Molar % with respect to total lipid, about 0.2 Molar % with respect to cholesterol) used in other experiments probing CBT-membrane interactions [70, 71, 80–82], the results from SANS and solid-state NMR require incorporation into current models for how pneumolysin and related toxins bring about pore formation and damage cells.

The structures of CBT oligomers

Cryo-electron microscopy (cryo-EM) is now a well-established means for directly observing macromolecular structures. Rapid freezing of the samples ensures that the solution conformation of the specimen is maintained; the images then obtained by transmission electron microscopy are two-dimensional electron density projections of the three-dimensional objects in the sample. By computationally determining the angular relationship of different projections, a full three-dimensional electron density map of the complex can be obtained. Hence, while fluorescence spectroscopy and solid-state NMR provide indirect information on structure by reporting the local environment of fluorescent or spin-labeled probes, cryo-EM provides direct information by imaging individual macromolecular complexes. Thus, although speculative thinking is likely to be involved in interpreting the mechanistic implications of a cryo-EM reconstruction – as it is in interpreting an X-ray crystal structure – the structure itself is a determined fact and, where combined with crystallographic data, can provide explicit descriptions of conformational changes undergone by molecules and their orientations in macromolecular assemblies. Recent examples of cryo-EM work include the pore-forming latrotoxin from the black widow spider [97], the U1 snRNP component of the spliceosome [98], the herpesvirus capsid at 8.5-Å resolution [99], and the structural dissection of membrane-containing alphaviruses including location of fusion proteins and their glycosylation sites [4, 5, 100].

Two conformations of CBT oligomers have been studied by cryo-EM. The first was the helical form of pneumolysin oligomer which forms at high toxin concentrations, and the second a membrane-bound form of oligomer [87]. The helical form was at higher resolution and provided a number of fundamental insights into CBT oligomerization (fig. 4a). First, this work demonstrated that the orientation in which the CBT monomer was modeled into an oligomer from the crystal structure, with domain 3 outwards and domain 2 forming the inner wall of the oligomer, was wrong [45]. Instead, domain 2 lines the outside of the oligomer and domains 3 and 4 project inwards. Second, this work revealed that oligomerization was accompanied by rotation of domain 4 upwards and appeared to involve conformational changes in domain 3 [87]. The membrane-bound form revealed a highly distinctive positioning of the oligomer above the membrane surface, connected by thin extensions, with the same orientation as in the helical oligomer but with the protein in a more similar conformation to the crystal structure (fig. 4b). The conformation of toxin found in the helix was initially proposed to be a precursor for forming that seen in the membrane-bound oligomer, which would be pore forming [87]. This speculation now appears in the light of

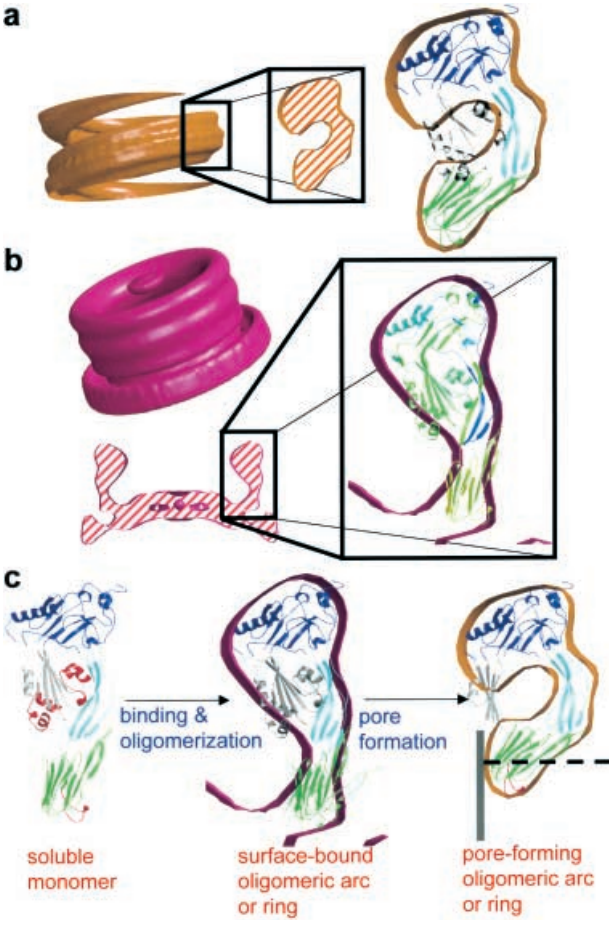

Figure 4. (*a*) The helical oligomeric form of pneumolysin. On the left, a single turn of the three-dimensional (3D) cryo-EM reconstruction is shown as an orange isosurface, with one edge boxed to highlight the section shown in the central panel. In the right-hand panel, the fit of domains from the perfringolysin crystal structure to this map is shown, with domain 1 colored blue, domain 2 cyan, domain 3 gray, and domain 4 green. (*b*) The surface-bound oligomeric form of pneumolysin. On the left, two views of the 3D cryo-EM reconstruction are shown: in the upper part, a tilted view of the whole map, in the lower part, a central section through it. On the right, the region boxed in the map section is shown with the perfringolysin crystal structure placed inside it. (*c*) Sequence of toxin conformations adopted during pore formation. The soluble monomer solved by X-ray crystallography is shown on the left. In the centre, the surface-bound oligomeric conformation is shown (as in b) with semi-transparent second copies of domains 2 and 4 to indicate some uncertainty about their positioning in the map and possible alternative orientations. This is the state referred to by Tweten and colleagues as the 'prepore.' On the right, the helical oligomeric conformation is shown, with semi-transparent domains again indicating some uncertainty in their positions. This conformation is suggested to be close to the pore-forming one. The small helices in domain 3 forming transmembrane regions of the pore-forming oligomer are not shown, and this domain has been rotated into a likely conformation in it. The putative transmembrane regions of domain 3 are marked schematically by a broad gray line, and the likely line of the membrane with a dashed line.

the work of Tweten and colleagues with perfringolysin to be wrong. In the same way, the oligomeric arrangment hypothesized for perfringolysin in the paper describing its monomeric structure was wrong [45]. The two pneumolysin cryo-EM maps define two conformations of CBT present in oligomers and there is no question about the correctness of the fitting of the perfringolysin crystal structure to the pneumolysin oligomer, revealing the orientation of CBTs within their oligomeric assemblies [87]. The membrane-bound oligomer encircled a region of membrane which still appeared intact [87] and should now be viewed as representing an intermediate oligomeric form occurring prior to pore formation (what Tweten and colleagues refer to as the 'prepore'). The structure of this form is very similar to that of the monomeric toxin, and shows that oligomerization in the absence of pore formation does not produce dramatic conformational changes in the structure of the protomer. In retrospect, this is unsurprising given that reversible self-interaction occurs in solution [83, 84]. Why pore formation did not occur in the liposomes used for preparing membrane-bound oligomers for cryo-EM analysis is unclear, but since the samples were generated at 20 °C, the fluidity of the membrane was possibly sufficiently reduced that the pore-forming regions of domain 3 could not partition into the bilayer. Another explanation is that successful pore formation is comparatively rare and that the pore-forming structures were missed in the cryo-electron micrographs. Observing membrane-bound oligomers which do not form pores means that CBTs can stably arrest at this point in their mechanism, which reiterates functional findings with reference to the action of streptolysin on fibroblasts and erythrocytes [101]. This reconstruction also provides direct structural evidence for a modest degree of membrane interaction on the part of domain 4 as surmised from fluorescence data [77, 78]. The lipid membrane displayed hollows on the outside of the surface-bound oligomer, and variations in electron density in the portion of the membrane circled by the toxin ring [87]. The chemical explanation for these structural features is unclear, although one might reasonably conclude that they relate to effects of the partial insertion of domain 4 on the membrane lipids. One stimulus for ordering of lipid components into definable structures observed by cryo-EM would be the redistribution of cholesterol as toxin protomer-cholesterol complexes self-associate into rings.

Although the conformation found in the helical form of pneumolysin oligomer was originally suggested to represent an intermediate on the way to the surface-bound oligomer just described, it seems now more likely to be closely related to that found in the toxin pore, since conformational changes which may be constrained by the lipid membrane at 20 °C can occur freely in solution. The work of Tweten and colleagues indicates that the changes in the conformation of domain 3 compared to the crystal structure arise from deployment of the helical regions which would associate with the membrane in β conformations but in the case of the helical toxin of course cannot. As a coda, CBT pores have now been observed by cryo-EM in liposome membranes [24].

The conformations of toxin molecules in both oligomeric forms are sufficiently distinctive that one can have a good degree of confidence in the general positioning and orientation of CBT molecules in these states, even if not in the precise positioning of individual domains. The ability to use cryo-EM to define the conformations of different oligomeric structures allows us to begin to escape rather schematic depictions of structural transitions in CBT-induced pore formation for explicit definitions of intermediate and final structures, as sketched out in figure 4c. A mechanism for CBT pore formation which is consistent with the data of both Tweten and Palmer (fig. 3c), incorporating the biochemical and biophysical data reviewed above with the structural insights provided by cryo-EM analyses, is as follows. The soluble monomer as defined by X-ray crystallography [45] binds to the membrane through its carboxy-terminal fourth domain, most likely directly via cholesterol but certainly in a cholesterol-dependent manner [44, 48, 57, 59, 60, 102]. The monomers bound to cholesterol skate about on the membrane surface, interacting primarily through the fourth domain of the protein [83–85]. Successful interaction through domains 4 leads to self-association of CBT protomers to form a dimer. Oligomerization continues either unidirectionally or bidirectionally, with the lengthening arc remaining in the conformation glimpsed in the surface-bound cryo-EM reconstruction [87] (fig. 4b). This stage in oligomerization terminates in pore formation, which occurs when regions of domain 3 insert into the membrane [70, 71, 79–82]. The surface-bound (prepore) toxin is metastable, and is poised to enter a lower energy state in forming a membrane-inserted pore-forming oligomer. Whether insertion and pore formation occurs with an arc or a ring will depend on how rapidly monomers can be recruited to the nascent oligomer (fig. 3c). The transition from surface-bound to membrane-inserted oligomer appears to be affected by the tryptophan within the conserved CBT undecapeptide (position 433 in pneumolysin) which when mutated to phenylalanine skews the pore size population toward the larger end of its range but reduces cytotoxicity by 99% [60]. The model being set out here suggests that substituting phenylalanine for tryptophan at this position may stabilize the surface-bound state and may reflect the same mechanism detected by Tweten and colleagues in the apparent influence of domain 4 on pore formation by domain 3 [81].

Although this scheme integrates the available data on pore formation by CBTs, it only serves to highlight ques-

tions for which as yet there are no clear answers. What is the structure of the portions of the membrane which complete pores formed by oligmeric CBT arcs? More particularly, what is the structure of the interface between the ends of the arc and the lipid? Assuming that domain 3 of each monomer provides two β hairpins to a giant β-sheeted structure which in oligomeric rings forms a huge β barrel [71, 80] poses a major question concerning pore-forming arcs: would they be stable structures, would the tensile strength of the arc be sufficient to maintain its curvature within a membrane? Or would pore-forming arcs indeed be short-lived structures nevertheless sufficient for the toxic purposes of the protein? Is it then particularly important to think in more dynamic terms about these toxins – and indeed about how they redistribute lipids in model systems [92, 93]? What is the molecular basis of the interaction between cholesterol and CBTs and is cholesterol actually their receptor [103]? How do current models for CBT activity relate to their suggested role as a system for injecting bacterial effector proteins into host cells [104]? What is the mechanism apparently linking domain 4 to pore formation by domain 3 [81] – and what has a tryptophan in the conserved CBT undecapeptide got to do with it [60]? What would more precisely determined structures for the surface-bound and pore-forming oligomeric toxin conformations reveal? Beginning to answer these questions using better attested mechanistic models and more detailed direct structural information on cholesterol-binding toxins is a major challenge for the immediate future.

Acknowledgements. The molecular structures and electron density maps in the figures were drawn using BOBSCRIPT [105–107] and rendered in RASTER3D [108]. The author is grateful to his coworkers with pneumolysin, particularly P. W. Andrew, B. B. Bonev, O. Byron, R. K. Heenan, J. L. Jiménez, P. J. Morgan, T. J. Mitchell, M. W. Parker, J. Rossjohn, H. R. Saibil, and A. Watts, and acknowledges the helpful comments of referees.

1 Bernheimer A. W. and Rudy B. (1986) Interactions between membranes and cytolytic peptides. Biochim. Biophys. Acta **864:** 123–141
2 Woolley G. A. and Wallace B. A. (1992) Model ion channels: gramicidin and alamethicin. J. Memb. Biol. **129:** 109–136
3 Bhakdi S. and Tranum-Jensen J. (1985) Complement activation and attack on autologous cell membranes induced by streptolysin-O. Infect. Immun. **48:** 713–719
4 Pletnev S. V., Zhang W., Mukhopadhyay S., Fisher B. R., Hernandez R., Brown D. T. et al. (2001) Locations of carbohydrate sites on alphavirus glycoproteins show that E1 forms an icosahedral scaffold. Cell **105:** 127–136
5 Lescar J., Roussel A., Wien M. W., Navaza J., Fuller S. D., Wengler G. et al. (2001) The fusion glycoprotein shell of semliki forest virus: an icosahedral assembly primed for fusogenic activation at endosomal pH. Cell **105:** 137–148
6 Song L. Z., Hobaugh M. R., Shustak C., Cheley S., Bayley H. and Gouaux J. E. (1996) Structure of staphylococcal alpha-hemolysin, a heptamertic transmembrane pore. Science **274:** 1859–1866
7 Gu L.Q., Braha O., Conlan S., Cheley S. and Bayley H. (1999) Stochastic sensing of organic analytes by a pore-forming protein containing a molecular adapter. Nature **398:** 686–690
8 Buchanan S. K., Smith B. S., Venkatramani L., Xia D., Esser L., Palnitkar M. et al. (1999) Crystal structure of the outer membrane active transporter FepA from *Escherichia coli.* Nat. Struct. Biol. **6:** 56–63
9 Gabriel K., Buchanan S. K. and Lithgow T. (2001) The alpha and the beta: protein translocation across mitochondrial and plastid outer membranes. Trends Biochem. Sci. **26:** 36–40
10 Koronakis V., Andersen C. and Hughes C. (2001) Channel-tunnels. Curr. Opin. Struct. Biol. **11:** 403–407
11 Koronakis V., Sharff A., Koronakis E., Luisi B. and Hughes C. (2000) Crystal structure of the bacterial membrane protein TolC central to multidrug efflux and protein export. Nature **405:** 914–919
12 Kuzmin P. I., Zimmerberg J., Chizmadzhev Y. A. and Cohen F. S. (2001) A quantitative model for membrane fusion based on low-energy intermediates. Proc. Natl. Acad. Sci. USA **98:** 7235–7240
13 Lentz B. R. and Lee J. K. (1999) Poly(ethylene glycol) (PEG)-mediated fusion between pure lipid bilayers: a mechanism in common with viral fusion and secretory vesicle release? Mol. Membr. Biol. **16:** 279–296
14 Peters C., Bayer M. J., Buhler S., Andersen J. S., Mann M. and Mayer A. (2001) Trans-complex formation by proteolipid channels in the terminal phase of membrane fusion. Nature **409:** 581–588
15 Gil T., Ipsen J. H., Mouritsen O. G., Sabra M. C., Sperotto M. M. and Zuckermann M. J. (1998) Theoretical analysis of protein organization in lipid membranes. Biochim. Biophys. Acta. **1376:** 245–266
16 Sousa M. V., Richardson M., Fontes W. and Morhy L. (1994) Homology between the seed cytolysin enterolobin and bacterial aerolysins. J. Protein Chem. **13:** 659–667
17 Fontes W., Sousa M. V., Aragao J. B. and Morhy L. (1997) Determination of the amino acid sequence of the plant cytolysin enterolobin. Arch. Biochem. Biophys. **347:** 201–207
18 Rossjohn J., Feil S. C., McKinstry W. J., Tsernoglou D., Goot G. van der, Buckley J. T. et al. (1998) Aerolysin – a paradigm for membrane insertion of beta-sheet protein toxins? J. Struct. Biol. **121:** 92–100
19 Bhakdi S., Bayley H., Valeva A., Walev I., Walker B., Weller U. et al. (1996) Staphylococcal alpha-toxin, streptolysin-O, and *Eschericia coli* hemolysin: prototypes of pore-forming bacterial cytolysins. Arch. Microbiol. **165:** 73–79
20 Hughson F. M. (1997) Penetrating insights into pore formation. Nat. Struct. Biol. **4:** 89–92
21 Lesieur C., Vecsey-Semjen B., Abrami L., Fivaz M. and Goot F. G. van der (1997) Membrane insertion: the strategies of toxins. Mol. Memb. Biol. **14:** 45–64
22 Gouaux E. (1997) Channel-forming toxins: tales of transformation. Curr. Opin. Struct. Biol. **7:** 566–573
23 Alouf J. E. (2001) Pore-forming bacterial protein toxins: an overview. Curr. Topics Microbiol. Immunol. **257:** 1–14
24 Gilbert R. J. C., Jimenez J. L., Chen S., Andrew P. W. and Saibil H. R. (2000) Structural basis of pore formation by cholesterol-binding toxins. Int. J. Med. Microbiol. **290:** 389–394
25 Merritt E. A. and Hol W. G. J. (1995) AB(5) toxins. Curr. Opin. Struct. Biol. **5:** 165–171
26 Stein P. E., Boodhoo A., Armstrong G. D., Cockle S. A., Klein M. H. and Read R. J. (1994) The crystal-structure of pertussis toxin. Structure **2:** 45–57
27 Vandenakker F., Sarfaty S., Twiddy E. M., Connell T. D., Holmes R. K. and Hol W. G. J. (1996) Crystal-structure of a new heat-labile enterotoxin, LT-IIb. Structure **4:** 665–678
28 Li J., Carroll J. and Ellar D. J. (1991) Crystal structure of insecticidal δ-endotoxin from *Bacillus thuringiensis* at 2.5 Å resolution. Nature **353:** 815–821

29 Griffitts J. S., Whitacre J. L., Stevens D. E. and Aroian R. V. (2001) Bt toxin resistance from loss of a putative carbohydrate-modifying enzyme. Science **293:** 860–864
30 Gahan L. J., Gould F. and Heckel D. G. (2001) Identification of a gene associated with Bt resistance in *Heliothis virescens.* Science **293:** 857–860
31 Lakey J. H. and Slatin S. L. (2001) Pore-forming colicins and their relatives. Curr. Topics Microbiol. Immunol. **257:** 131–161
32 Parker M. W. (1997) More than one way to make a hole. Nat. Struct. Biol. **4:** 250–253
33 Rossjohn J., Feil S. C., McKinstry W. J., Tsernoglou D., Goot F. G. van der, Buckley J. T. et al. (1998) Aerolysin – a paradigm for membrane insertion of beta-sheet protein toxins? J. Struct. Biol. **121:** 92–100
34 Heuck A. P., Tweten R. K. and Johnson A. E. (2001) β-Barrel pore-forming toxins: intriguing dimorphic proteins. Biochemistry **40:** 9065–9073
35 Petosa C., Collier R. J., Klimpel K. R., Leppla S. H. and Liddington R. C. (1997) Crystal structure of the anthrax toxin protective antigen. Nature **385:** 833–838
36 Parker M. W., Buckley J. T., Postma J. P. M., Tucker A. D., Leonard K., Pattus F. et al. (1994) Structure of the *Aeromonas* toxin proaerolysin in its water-soluble and membrane-channel states. Nature **367:** 292–295
37 Pedelacq J. D., Maveyraud L., Prevost G., Baba-Moussa L., Gonzalez A., Courcelle E. et al. (1999) The structure of a *Staphylococcus aureus* luecocidin component (LukF-PV) revelas the fold of the water-soluble species of a family of transmembrane pore-forming toxins. Structure **7:** 277–287
38 Olson R., Nariya H., Yokota K., Kamio Y. and Gouaux E. (1999) Crystal structure of staphylococcal LukF delineates conformational changes accompanying formation of a transmembrane channel. Nat. Struct. Biol. **6:** 134–140
39 Miles G., Cheley S., Braha O. and Bayley H. (2001) The staphylococcal leukocidin bicomponent toxin forms large ionic channels. Biochemistry **40:** 8514–8522
40 Smart O. S., Coats G. M. P., Sansom M. S. P., Aldwer G. M. and Bashford C. L. (1999) Structure-based prediction of the conductance properties of ion channels. Faraday Discuss. **111:** 185–199
41 Klug A. (1969) Point groups and the design of aggregates. In: Nobel Symposium 11: Symmetry and Function of Biological Systems at the Macromolecular Level, pp. 425–436, Engström A. and Strandberg B. (eds), Wiley, London
42 Movileanu L., Howorka S., Braha O. and Bayley H. (2000) Detecting protein analytes that modulate transmembrane movement of a polymer chain within a single protein pore. Nat. Biotechnol. **18:** 1091–1095
43 Howorka S., Cheley S. and Bayley H. (2001) Sequence-specific detection of individual DNA strands using engineered nanopores. Nat. Biotechnol. **19:** 636–639
44 Tweten R. K., Parker M. W. and Johnson A. E. (2001) The cholesterol-dependent cytolysins. Curr. Topics Microbiol. Immunol. **257:** 15–33
45 Rossjohn J., Feil S. C., McKinstry W. J., Tweten R. K. and Parker M. W. (1997) Structure of a cholesterol-binding, thiol-activated cytolysin and a model of its membrane form. Cell **89:** 685–692
46 Atkins A., Wyborn N. R., Wallace A. J., Stillman T. J., Black L. K., Fielding A. B. et al. (2000) Structure-function relationships of a novel bacterial toxin, hemolysin E: the role of alpha G. J. Biol. Chem. **275:** 41150–41155
47 Wallace A. J., Stillman T. J., Atkins A., Jamieson S. J., Bullough P. A., Green J. et al. (2000) *E. coli* hemolysin E (HlyE, ClyA, SheA): X-ray crystal structure of the toxin and observation of membrane pores by electron microscopy. Cell **100:** 265–276
48 Alouf J. E. and Geoffroy C. (1991) The family of the antigenically-related, cholesterol-binding ('sulphydryl-activated') cytolytic toxins. In: Sourcebook of Bacterial Protein Toxins, pp. 147–186, Freer J. H. (ed.), Academic Press, London
49 Billington S. J., Josy B. H., Cuevas W. A., Bright K. R. and Songer J. G. (1997) The *Arcanobacterium* (*Actinomyces*) *pyogenes* hemolysin, pyolysin, is a novel member of the thiol-activated cytolysin family. J. Bacteriol. **179:** 6100–6106
50 Alouf J. E. (2000) Cholesterol-binding cytolytic protein toxins. Int. J. Med. Microbiol. **290:** 351–356
51 Morgan P. J., Andrew P. W. and Mitchell T. J. (1996) Thiol-activated cytolysins. Rev. Med. Microbiol. **7:** 221–229
52 Walev I., Bhakdi S. C., Hofmann F., Djonder N., Valeva A., Aktories K. et al. (2001) Delivery of proteins into living cells by reversible membrane permeabilization with streptolysin-O. Proc. Natl. Acad. Sci. USA **98:** 3185–3190
53 Weiglein I., Goebel W., Troppmair J., Rapp U. R., Demuth A. and Kuhn M. (1997) *Listeria monocytogenes* infection of HeLa cells results in listeriolysin O-mediated transient activation of the Raf-MEK-MAP kinase pathway. FEMS Microbiol. Lett. **148:** 189–195
54 Jones S. and Portnoy D. A. (1994) Characterization of *Listeria monocytogenes* pathogenesis in a strain expressing perfringolysin-O in place of listeriolysin-O. Infect. Immun. **62:** 5608–5613
55 Jones S., Preiter K. and Portnoy D. A. (1996) Conversion of an extracellular cytolysin into a phagosome-specific lysin which supports the growth of an intracellular pathogen. Mol. Microbiol. **21:** 1219–1225
56 Rottem S., Hardegree M. C., Grabowski M. W., Fornwald R. and Barile M. F. (1976) Interaction between tetanolysin and mycoplasma cell membrane. Biochim. Biophys. Acta **455:** 876–888
57 Bernheimer A. (1972) Hemolysis of streptococci: characterization and effects on biological membranes. In: The Streptococci and Streptococcal Diseases: Recognition, Understanding and Management, pp. 19–31, Matsen J. M. (ed.), Academic Press, London
58 Harris J. R., Adrian M., Bhakdi S. and Palmer M. (1998) Cholesterol-streptolysin O interaction: an EM study of wild-type and mutant streptolysin O. J. Struct. Biol. **121:** 343–355
59 Alving C. R., Habig W. H., Urban K. A. and Hardegree M. C. (1979) Cholesterol-dependent tetanolysin damage to liposome. Biochim. Biophys. Acta **551:** 224–228
60 Korchev Y. E., Bashford C. L., Pederzolli C., Pasternak C. A., Morgan P. J., Andrew P. W. et al. (1998) A conserved tryptophan in pneumolysin is a determinant of the characteristics of channels formed by pneumolysin in cells and planar lipid bilayers. Biochem. J. **329:** 571–577
61 Ohno-Iwashita Y., Iwamoto M., Mitsui K.-I., Ando S. and Iwashita S. (1991) A cytolysin, θ-toxin, preferentially binds to membrane cholesterol surrounded by phospholipids with 18-carbon hydrocarbon chains in cholesterol-rich region. J. Biochem. **110:** 369–375
62 Ohno-Iwashita Y., Iwamoto M., Ando S. and Iwashita S. (1992) Effect of lipidic factors on membrane cholesterol topology – mode of binding of θ-toxin to cholesterol liposomes. Biochim. Biophys. Acta **1109:** 81–90
63 Delattre J., Badin J., Canal J. and Girard M. L. (1973) Influence des lecithines sur le pouvoir inhibiteur du cholesterol visa-vis de la streptolysine O. C. R. Acad. Sci. D **277:** 441–443
64 Fujii G., Chang J.-E., Coley T. and Steere B. (1997) The formation of amphotericin B ion channels in lipid bilayers. Biochemistry **36:** 4959–4968
65 Behnke O., Tranum-Jensen J. and Deurs B. von (1984) Filipin as a cholesterol probe. I. Morphology of filipin-cholesterol interaction in lipid model systems. Eur. J. Cell Biol. **35:** 189–199
66 Behnke O., Tranum-Jensen J. and Deurs B. von (1984) Filipin as a cholesterol probe. II. Filipin-cholesterol interaction in red blood cell membranes. Eur. J. Cell Biol. **35:** 200–215

67 Bhakdi S., Tranum-Jensen J. and Sziegoleit A. (1985) Mechanism of membrane damage by streptolysin-O. Infect. Immun. **47:** 52–60

68 Morgan P. J., Hyman S. C., Byron O., Andrew P. W., Mitchell T. J. and Rowe A. J. (1994) Modeling the bacterial protein toxin, pneumolysin, in its monomeric and oligomeric form. J. Biol. Chem. **269:** 25315–25320

69 Palmer M., Harris R., Freytag C., Kehoe M., Tranum-Jensen J. and Bhakdi S. (1998) Assembly mechanism of the oligomeric streptolysin O pore: the early membrane lesion is lined by a free edge of the lipid membrane and is extended gradually during oligomerization. EMBO J. **17:** 1598–1605

70 Hotze E. M., Wilson-Kubalek E. M., Rossjohn J., Parker M. W., Johnson A. E. and Tweten R. K. (2001) Arresting pore formation of a cholesterol-dependent cytolysin by disulfide trapping synchronizes the insertion of the transmembrane beta-sheet from a prepore intermediate. J. Biol. Chem. **276:** 8261–8268

71 Shatursky O., Heuck A. P., Shepard L. A., Rossjohn J., Parker M. W., Johnson A. E. et al. (1999) The mechanism of membrane insertion for a cholesterol-dependent cytolysin: a novel paradigm for pore-forming toxins. Cell **99:** 293–299

72 Hill J., Andrew P. W. and Mitchell T. J. (1994) Amino acids in pneumolysin important for hemolytic activity identified by random mutagenesis. Infect. Immun. **62:** 757–758

73 Pinkney M., Beachey E. and Kehoe M. (1989) The thiol-activated toxin streptolysin O does not require a thiol group for cytolytic activity. Infect. Immun. **57:** 2553–2558

74 Sekino-Suzuki N., Nakamura M., Mitsui K.-I. and Ohno-Iwashita Y. (1996) Contribution of individual tryptophan residues to the structure and activity of θ-toxin (perfringolysin O), a cholesterol-binding cytolysin. Eur. J. Biochem. **241:** 941–947

75 Saunders F. K., Mitchell T. J., Walker J. A., Andrew P. W. and Boulnois G. J. (1989) Pneumolysin, the thiol-activated toxin of *Streptococcus pneumoniae*, does not require a thiol group for in vitro activity. Infect. Immun. **57:** 2547–2552

76 Rossjohn J., Gilbert R. J. C., Crane D., Morgan P. J., Mitchell T. J., Rowe A. J. et al. (1998) The molecular mechanism of pneumolysin, a virulence factor from *Streptococcus pneumoniae.* J. Mol. Biol. **284:** 449–461

77 Nakamura M., Sekino N., Iwamoto M. and Ohno-Iwashita Y. (1995) Interaction of θ-toxin (perfringolysin O), a cholesterol-binding cytolysin, with liposomal membranes: change in the aromatic side chains upon binding and insertion. Biochemistry **34:** 6513–6520

78 Nakamura M., Sekino-Suzuki N., Mitsui K.-I. and Ohno-Iwashita Y. (1998) Contribution of tryptophan residues to the structural changes in perfringolysin O during interaction with liposomal membranes. J. Biochem. **123:** 1145–1155

79 Palmer M., Saweljew P., Vulicevic I., Valeva A., Kehoe M. and Bhakdi S. (1996) Membrane-penetrating domain of streptolysin O identified by cysteine scanning mutagenesis. J. Biol. Chem. **271:** 26664–26667

80 Shepard L. A., Heuck A. P., Hamman B. D., Rossjohn J., Parker M. W., Ryan K. R. et al. (1998) Identification of a membrane-spanning domain of the thiol-activated pore-forming toxin *Clostridium perfringens* perfringolysin O: an α-helical to β-sheet transition identified by fluorescence spectroscopy. Biochemistry **37:** 14563–14574

81 Heuck A. P., Hotze E. M., Tweten R. K. and Johnson A. E. (2000) Mechanism of membrane insertion of a multimeric beta-barrel protein: perfringolysin O creates a pore using ordered and coupled conformational changes. Mol. Cell **6:** 1233–1242

82 Shepard L. A., Shatursky O., Johnson A. E. and Tweten R. K. (2000) The mechanism of pore assembly for a cholesterol-dependent cytolysin: formation of a large prepore complex precedes the insertion of the transmembrane beta-hairpins. Biochemistry **39:** 10284–10293

83 Gilbert R. J. C., Rossjohn J., Parker M. W., Tweten R. K., Morgan P. J., Mitchell T. J. et al. (1998) Self-interaction of pneumolysin, the pore forming protein toxin of *Streptococcus pneumoniae.* J. Mol. Biol. **284:** 1223–1237

84 Gilbert R. J. C., Heenan R. K., Timmins P. A., Gingles N. A., Mitchell T. J., Rowe A. J. et al. (1999) Studies on the structure and mechanism of a bacterial protein toxin by analytical ultracentrifugation and small-angle neutron scattering. J. Mol. Biol. **293:** 1145–1160

85 Weis S. and Palmer M. (2001) Streptolysin O: the C-terminal, tryptophan-rich domain carries functional sites for both membrane binding and self-interaction but not for stable oligomerization. Biochim. Biophys. Acta **1510:** 292–299

86 Mitchell T. J., Andrew P. W., Saunders F. K., Smith A. N. and Boulnois G. J. (1991) Complement activation and antibody binding by pneumolysin via a region of the toxin homologous to a human acute-phase protein. Mol. Microbiol. **5:** 1883–1888

87 Gilbert R. J. C., Jimenez J. L., Chen S., Tickle I. J., Rossjohn J., Parker M. W. et al. (1999) Two structural transitions in membrane pore formation by pneumolysin, the pore-forming toxin of *Streptococcus pneumoniae.* Cell **97:** 647–655

88 Menestrina G., Bashford C. L. and Pasternak C. A. (1990) Pore-forming toxins: experiments with *S. aureus* α-toxin, *C. perfringens* θ-toxin and *E. coli* hemolysin in lipid bilayers, liposomes and intact cells. Toxicon **28:** 477–491

89 Korchev Y. E., Bashford C. L. and Pasternak C. A. (1992) Differential sensitivity of pneumolysin-induced channels to gating by divalent cations. J. Memb. Biol. **127:** 195–203

90 Auger M. (2000) Biological membrane structure by solid-state NMR. Curr. Issues Mol. Biol. **2:** 119–124

91 Satoh O., Imai H., Yoneyama T., Miyamura T., Utsumi H., Inoue K. et al. (2000) Membrane structure of the hepatitis B virus surface antigen particle. J. Biochem. **127:** 543–550

92 Bonev B., Gilbert R. J. C. and Watts A. (2000) Structural investigations of pneumolysin/lipid complexes. Mol. Memb. Biol. **17:** 229–235

93 Bonev B. B., Gilbert R. J. C., Andrew P. W., Byron O. and Watts A. (2001) Structural analysis of the protein/lipid complexes associated with pore formation by the bacterial toxin pneumolysin. J. Biol. Chem. **276:** 5714–5719

94 Zitzer A., Bittman R., Verbicky C. A., Erukulla R. K., Bhakdi S., Weis S. et al. (2001) Coupling of cholesterol and cone-shaped lipids in bilayers augments membrane permeabilization by the cholesterol-specific toxins streptolysin O and *Vibrio cholerae* cytolysin. J. Biol. Chem. **276:** 14628–14633

95 Seddon J. M. (1990) Structure of the inverted hexagonal (HII) phase, and non lamellar phase transitions of lipids. Biochim. Biophys. Acta **1031:** 1–69

96 Killian J. A., Salemink I., Planque M. R. R. de, Lindblom G., Koepe R. E. II and Greathouse D. V. (1996) Induction of nonbilayer structures in diacylphosphocholine model membranes by transmembrane [alpha]-helical peptides: importance of hydrophobic mismatch and proposed role of tryptophans. Biochemistry **35:** 1037–1045

97 Orlova E. V., Rahman M. A., Gowen B., Volynski K. E., Ashton A. C., Manser C. et al. (2000) Structure of alpha-latrotoxin oligomers reveals that divalent cation-dependent tetramers form membrane pores. Nat. Struct. Biol. **7:** 48–53

98 Stark H., Dube P., Luhrmann R. and Kastner B. (2001) Arrangement of RNA and proteins in the spliceosomal U1 small nuclear ribonucleoprotein particle. Nature **409:** 539–542

99 Zhou Z. H., Dougherty M., Jakana J., He J., Rixon F. J. and Chiu W. (2000) Seeing the herpesvirus capsid at 8.5 Å. Science **288:** 877–880

100 Mancini E. J., Clarke M., Gowen B. E., Rutten T. and Fuller S. D. (2000) Cryo-electron microscopy reveals the functional organization of an enveloped virus, Semliki Forest virus. Mol. Cell **5:** 255–266
101 Walev I., Palmer M., Valeva A., Weler U. and Bhakdi S. (1995) Binding, oligomerization, and pore formation by streptolysin O in erythrocytes and fibroblast membranes: detection of nonlytic polymers. Infect. Immun. **63:** 1188–1194
102 Rottem S., Cole R. M., Habig W. H., Baile M. H. and Hardegree M. C. (1982) Structural characteristics of tetanolysin and its binding to lipid vesicles. J. Bacteriol. **152:** 888–892
103 Jacobs T., Darji A., Frahm N., Rohde M., Wehland J., Chakraborty T. et al. (1998) Listeriolysin O: cholesterol inhibits cytolysis but not binding to cellular membranes. Mol. Microbiol. **28:** 1081–1089
104 Madden J. C., Ruiz N. and Caparon M. (2001) Cytolysin-mediated translocation (CMT): a functional equivalent of type III secretion in gram-positive bacteria. Cell **104:** 143–152
105 Kraulis P. J. (1991) MOLSCRIPT – a program to produce both detailed and schematic plots of protein structures. J. Appl. Crystallogr. **24:** 946–950
106 Esnouf R. M. (1997) An extensively modified version of Molscript that includes greatly enhanced colouring capabilities. J. Mol. Graph. **15:** 132–134
107 Esnouf R. M. (1999) Further additions to MolScript version 1.4, including reading and contouring of electron-density maps. Acta Crystallogr. D **55:** 938–940
108 Merritt E. A. and Murphy M. E. P. (1994) Raster3D version 2.0: a program for photorealistic molecular graphics. Acta Crystallogr. D **50:** 869–873